BMC Microbiology

RESEARCH

Open Access

Characterization of the *Priestia megaterium* ZS-3 siderophore and studies on its growth-promoting effects

Xiao-Xia Zhu[1,2†], Li-Na Shi[1,2†], Hui-Min Shi[1,2] and Jian-Ren Ye[1,2*]

Abstract

Background The ability of plant growth-promoting rhizobacteria (PGPR) to alleviate iron deficiency-induced chlorosis in plants has been widely reported, but the role of siderophores in the re-greening process has rarely been investigated. In this study, the *Priestia megaterium* ZS-3 (ZS-3) siderophore was first characterized, and a 100-fold concentration of the crude extract of the siderophore was extracted by solid-phase extraction and used to inoculate *Arabidopsis thaliana* to investigate whether the ZS-3 siderophore could alleviate plant iron deficiency-induced chlorosis in the presence of an insoluble iron source and to determine how it promoted plant growth.

Results The results indicated that -Fe + Fe_2O_3 (Fe_2O_3) treatment induced a decrease in plant growth and iron nutritional status compared with those in the 1/2 MS (one-half-strength Murashige and Skoog medium). Expression levels of representative genes for chlorophyll synthesis, *CHLM* and *CHLG*, increased by 85.41% and 77.05% compared to Fe_2O_3 treatment; the *IRT1* and *FRO*$_2$ in Fe_2O_3 inoculated with the ZS-3 siderophore (T2 treatment) were upregulated by 88.1% and 87.20%, respectively. These results indicate that the ZS-3 siderophore upregulates the expressions of chlorophyll genes to increases photosynthesis and helps plants increase the transcription of iron and the activity of ferric-chelate reductase. Compared with the Fe_2O_3 treatment, the T2 group increased the soluble protein and chlorophyll contents by 2.64- and 3.47-fold, and improved the activities of ferric-chelate reductase and peroxidase (POD) by 3.69- and 2.9-fold, respectively, indicating that the ZS-3 siderophore maintained normal plant growth under Fe_2O_3 stress by increasing the activity of antioxidant enzymes.

Conclusions This study revealed that the ZS-3 siderophore Ferrioxamine E [M + Fe-2 H] enhances plant iron uptake and transport activity at the transcriptional level, confirming the important role of the ZS-3 siderophore in plant iron deficiency status, and the results suggest that the ZS-3 siderophore helps plants acquire iron, alleviates plant chlorosis and promotes plant growth through mechanism I of plant iron acquisition. In this study, we closely linked the structural characterization and quantification of siderophores with Fe deficiency-induced chlorosis to elucidate the promotional mechanism of siderophores in Fe-deficient environments.

Keywords *Priestia megaterium*, Siderophore, Promote growth, Characterization, Chlorosis

†Xiao-Xia Zhu and Li-Na Shi contributed equally to this work.

*Correspondence:
Jian-Ren Ye
njfu_jrye@163.com

[1]Co-Innovation Center for Sustainable Forestry in Southern China, College of Forestry, Nanjing Forestry University, Nanjing 210037, Jiangsu, China
[2]Jiangsu Key Laboratory for Prevention and Management of Invasive Species, Nanjing Forestry University, Nanjing 210037, Jiangsu, China

Introduction

Iron is an essential element for the growth and metabolism of organisms and plays a core role in photosynthesis, respiration, and DNA synthesis and repair [1, 2]. Approximately 4,600 iron atoms are stored in each molecule of ferritin in the chloroplast matrix [3], and more than 80% of the iron in plants is distributed among the leaf cells [4]. Iron deficiency is associated with a decrease in the grana lamella of the thylakoid, and chloroplasts disintegrate in severe cases of iron deficiency, which greatly inhibits photosynthesis, delays plant development and reduces nutrient accumulation [5]. The soil does not lack iron, but rather, a high soil pH limits the availability of iron, resulting in most of the iron sources being in the form of Fe_2O_3 in the soil; this form cannot be directly absorbed and utilized by plants [6]. As a result, plants develop different strategies to survive in iron-deficient environments. Most dicotyledonous and nongramineous monocotyledonous plants obtain iron through mechanism I; that is, after being activated by the induction of an iron deficiency, the proton pump in the plasma membrane of plant roots secretes H^+, reduces the rhizosphere soil pH and increases the solubility of Fe (III), which is converted into Fe (II) through ferric-chelate reductase (FCR) on the root cell membrane, and then Fe (II) is transported to plant cells. In *A. thaliana*, H^+-ATPase is encoded by the *AHA* gene, which is induced by iron deficiency and is primarily responsible for the process of secreting H^+ [7, 8]. *AtFRO*$_2$ is the most important gene among the 8 ferric chelate reductase (FRO) genes involved in iron reduction processes [8, 9]. *AtIRT1* is involved in Fe (II) transport in *A. thaliana*, and *irt1* mutants exhibit severe chlorosis and seedling mortality due to iron deficiency; therefore, *IRT1* is essential for plant Fe (II) uptake [9, 10]. Plants that obtain iron through mechanism II are mainly monocotyledonous gramineous plants that release chelators into the soil to bind to Fe (III), forming a soluble complex that is absorbed by the root plasma membrane [11]. Although plants have evolved various physiological strategies to enhance their ability to tolerate iron deficiency, in soils with severe iron deficiency, plants cannot fully overcome this deficiency by relying on the above two mechanisms alone.

In response to the stress of iron deficiency in nature, organisms have evolved the ability to produce highly specific iron chelators called siderophores [12, 13]. Siderophores are small molecule compounds that bind specifically to Fe (III) with heterogeneous groups of ligands and are highly specific and selective [1, 14]. The stability constant of siderophores that bind to Fe (III) is usually greater than 10^{30} [15]. Siderophores are classified into the hydroxamic acid type, catechol type, α-carboxylic acid type and mixed type according to their functional groups that bind to iron atoms. Among them, mixed-type siderophores contain more than one type of iron coordination group [3]. Generally, the central ions of the coordination groups have six-coordinated octahedral geometries, such as bacillibactin (catecholic type) produced by *Bacillus anthracis* [16], vicibactin (cyclic hydroxamic acid type) from *Rhizobium* [17], rhizoferrin (α-carboxylic acid type) from *Francisella tularensis*, and pyoverdines (mixed type) from *Pseudomonas* [3]. Several studies have shown that siderophores are one of the important direct promoting mechanisms of PGPR [18–20], and the application of siderophore-producing PGPR can mitigate leaf chlorosis and has a growth-promoting effect in iron-deficient environments. Stuti Sah used *Pseudomonas aeruginosa* RSP5 as an inoculant for iron translocation in maize and reported that RSP5 increased the iron content in maize stems, leaves and seeds and alleviated plant chlorosis in iron-deficient soil environments [21]. Yue cocultivated the siderophore-producing bacterium WR12 with wheat in iron-deficient hydroponic nutrient solution, and compared with the control, WR12 significantly increased the chlorophyll content and wheat iron content [5]. All of these studies indicate that PGPR, which can produce siderophores, play an important role in plant growth, but it is not clear how siderophores activate plant iron regulatory transcripts to help plants obtain iron.

Priestia megaterium is a class of PGPR that has received much attention because of its unique physiological metabolism, harmlessness to humans and animals, and safety for food crops [22, 23]. The original scientific name of *Priestia megaterium* was *Bacillus megaterium*, which was renamed *Priestia megaterium* by Gupta et al. through phylogenomic and comparative genomic analyses in 2020 [24]; since then, scholars have gradually used this new scientific name. From 1984 to 1995, Jeffrey E. Plowman, Xicheng Hu, and Hataichanok Chuljerm successively characterized the production of various siderophores by various strains of this group, such as schizokinen, schizokinen A, N deoxyschizokinen and schizokinen imide [13, 25], which all belong to the schizokinen family, among which schizokinen binds specifically to gallium (III) and has considerable potential in the development of medical clinical diagnostic reagents. At present, no other types of siderophiles or their applications have been reported in strains of *Priestia megaterium*.

P. megaterium ZS-3 is an excellent growth-promoting strain screened by the Forest Pathology Laboratory of Nanjing Forestry University [23, 26]. Previous studies have shown that ZS-3 has a strong ability to produce siderophores (experimental data not published). Therefore, the purpose of this study was to characterize the siderophore structure of *P. megaterium* ZS-3, to analyze the causes and mechanisms of iron deficiency-induced

chlorosis in plants on the basis of previous theoretical studies and to reveal how the ZS-3 siderophore alleviates iron deficiency chlorosis and promotes plant growth. To clarify the significance of siderophores in maintaining normal plant growth and alleviating leaf chlorosis under iron deficiency conditions, we further confirmed the effect of siderophores on plant growth and laid a theoretical foundation for further research on the transport mechanism of siderophore-Fe in plants.

Materials and methods

Preparation of the fermentation solution for strains

P. megaterium ZS-3 (Preservation of Chinese Typical Culture Collection Centre, Wuhan, China) (Collection No. CCTCC M 20231406) and *Rahnella aquatilis* JZ-GX1 (Collection No. CCTCC M 2012439) were inoculated in Luria–Bertani (LB) medium overnight at 28 °C in a shaker. Then, the bacterial cells were collected, washed twice with an equal volume of 1× PBS buffer (Solarbio, Beijing, China), inoculated with a 1% volume of iron-restricted sucrose-asparagine (MSA) liquid medium, and incubated in a shaker at 28 ℃ for 36 h to obtain the fermentation broths of ZS-3 and JZ-GX1. Modified MSA medium was used to induce the secretion of siderophores by ZS-3 and JZ-GX1. The MSA consisted of 20 g sucrose, 2 g L-asparagine, 1 g K_2HPO_4, and 0.5 g $MgSO_4{\cdot}7H_2O$ per liter.

Identification of siderophore types

The bacterial fermentation broth was centrifuged to obtain the supernatant, which was passed through a 0.22 μm microporous filter membrane and then prepared for use. Catechol-type siderophores were detected by Arnow's test and the $FeCl_3$ test, carboxylic acid-type siderophores were detected by the spectrophotometric test, and hydroxamic acid-type siderophores were detected by the $FeCl_3$ test and tetrazolium test, both of which refer to the methods reported by Arefa Baakza [27].

Preparation of the crude siderophore extract

The strains were incubated in MSA media at 28 ℃ and 200 rpm for 36 h, centrifuged at 8000 rpm for 15 min, and passed through a 0.22 μm bacterial filter membrane. One hundred milliliters of supernatant was extracted from a C_{18} column (Supelco, Bellefonte, America) by solid phase extraction (column type SLBC1810300), eluted with 1 mL of 60% methanol, and concentrated 100-fold. Forty microliters of crude extract was applied to a chrome azurol sulfonate (CAS) agar plate (Coolaber, Beijing, China) for color reaction, and the siderophore ring was observed overnight.

Structural characterization of the *P. megaterium* ZS-3 siderophore

To determine the chemical structure of the ZS-3 100-fold crude extract compounds, liquid chromatography tandem mass spectrometry (LC–MS/MS) was performed. The samples were subjected to ultrahigh liquid chromatography (Nexera UHPLC LC-30 A, Shimadzu, Japan) and mass spectrometry (AB SCIEX™ TripleTOF5600+, Washington, USA). The siderophore extract was separated on a Sepax GP-C_{18} column (1.8 μm, 120 A, 2.1 mm*150 mm) as the stationary phase and 0.1% formic acid and 100% acetonitrile as the mobile phase at a flow rate of 0.3 mL/min with a detection test column temperature of 40 ℃ and a 21 min analysis time for each component.

Mass spectrometric detection was carried out using electrospray ionization (ESI) in positive and negative ion modes. The detection of selected ions was carried out in ESI mode with ion source gas 1 (gas 1):50, gas 2:50 and curtain gas:25 with a source temperature of 500 °C (positive ion mode) and 450 °C (negative ion mode). ESI mode analyses were performed with ion spray voltage floating at 5500 V (positive ion mode) and 4400 V (negative ion mode), a 100–1200 Da TOF MS scan range and a 50-1000 Da product ion scan range. The TOF MS scan accumulation time and product ion scan accumulation time were 0.2 s and 0.01 s, respectively. The secondary mass spectra were obtained by information-dependent acquisition in high-sensitivity mode.

P. megaterium ZS-3 quantitative assay of crude siderophore extracts

The quantitative operation of the crude extraction of siderophores concentrated 100-fold refers to the preparation of the crude extracts mentioned above. Quantitative analysis was performed after 36 h of cultivation with 3 samples ($n = 3$). LC–MS/MS was used to quantify the siderophore content in the 100-fold crude extract of ZS-3. Detection was performed on an Agilent C_{18} 1290–6470 column (2.1 mm×100 mm, 1.8 μm) (Agilent, Palo Alto, America) as the stationary phase and with pure water (containing 0.1% formic acid) and acetonitrile (containing 0.1% formic acid) as the mobile phase at a flow rate of 0.3 mL/min with a detection test column temperature of 35 ℃ and an injection volume of 2 μL.

Plant materials and treatments

A. thaliana ecotype Columbia-0 (Col-0) seeds were disinfected according to the method reported by Shi, LN [23]. All plates were stored at 4 °C in the dark for 48 h to ensure vernalization. Five days after germination, the plants were transferred to different media and subjected to a photoperiod of 16 h/8 h and a culture temperature of 22 ± 2 °C. A total of 7 groups were set up in

the experiment: one-half-strength Murashige and Skoog medium (1/2 MS), 1/2 MS—Fe (here after represented by –Fe) (Coolaber, Beijing, China); 1/2 MS–Fe + Fe_2O_3 (100 ml medium + 0.05 g Fe_2O_3, represented by Fe_2O_3); 1/2 MS–Fe + Fe_2O_3 + siderophore crude extract (100 ml medium + 500 μL crude extract, represented by T1); T2: 1/2 MS–Fe + Fe_2O_3 + siderophore (100 ml medium + 1 mL crude extract, represented by T2); 1/2 MS–Fe + Fe_2O_3 + siderophore (100 ml medium + 3 mL crude extract, represented by T3); and 1/2 MS–Fe + Fe_2O_3 + siderophore (100 ml medium + 5 mL crude extract, represented by T4).

Growth and biomass yield

The superoxide dismutase (SOD) and peroxidase (POD) activities, hydrogen peroxide (H_2O_2) content, and malondialdehyde (MDA) content were measured in 0.1 g of fresh leaves; the ferric chelator reductase (FCR) activity was measured in 0.1 g of fresh plant roots; and the protein and active iron contents were measured in 0.1 g of whole plants. All absorbance readings were determined with a Multiskan Spectrum instrument (Thermo, USA). Plants were cultured under different treatments for 15 days to determine the growth indicators.

For protein, POD, SOD and FCR, plant tissue was homogenized in an ice bath with distilled water (1 mL). The resulting homogenate was centrifuged at 10,000 rpm for 10 min at 4 °C.

The protein content (mg/g) was determined with a protein kit (Comin, Suzhou, China). The absorbance was recorded at 562 nm.

The peroxidase (POD) activity (U g^{-1} FW) of fresh leaves was assayed with a POD kit (Comin, Suzhou, China). The absorbance was read at 470 nm.

Superoxide dismutase (SOD) activity (U g^{-1} FW) was determined by a nitrogen blue tetrazole (NBT) photochemical reduction kit (Comin, Suzhou, China). The absorbance was recorded at 560 nm.

The ferric-chelate reductase (FCR) activity (nmol/min/g) of the plant roots was determined according to the instructions of the ferric-chelate reductase kit (Comin, Suzhou, China). The absorbance was read at 562 nm.

The hydrogen peroxide (H_2O_2) content was determined by an H_2O_2 kit (Comin, Suzhou, China) with acetone as the extraction solution. The resulting homogenate was centrifuged at 10,000 rpm for 10 min at 4 °C, and the absorbance was recorded at 415 nm.

The plant fresh weight was measured by an analytical scale, and the length of the main roots of the plants was measured with a ruler. Fourteen plants were taken from each group, and the mean values were determined.

The malondialdehyde (MDA) content in the leaves was measured according to the method reported by Kumar [28]. The plant leaves were homogenized in 1 mL of thiobarbituric acid (0.25%, w/v) in 10% (w/v) trichloroacetic acid (TCA). The homogenates were incubated at high temperature for half an hour and then centrifuged at 10,000 rpm for 20 min. Absorbance was measured at 450 and 532 nm. The MDA content was calculated according to the following equation:

$$\mathrm{MDA}\ \left(\mu\,\mathrm{mol\,g^{-1}FW}\right) = (6.45 \times\ \mathrm{OD_{532}}) - (0.56 \times\ \mathrm{OD_{450}})$$

The determination of the chlorophyll content was based on the method reported by Azarmi et al. [29]. Leaf samples were cut into pieces (0.1 g) and ground with a small amount of acetone. Then, 10 mL of acetone was added, and the samples were fixed and kept in the dark overnight until the next day, when the residue turned completely white. The absorbance was recorded at 663.6, 646.6 and 470 nm (Thermo, USA) to quantify the chlorophyll content.

$$\mathrm{Chl.a\ (g/mL\ FW)} = 12.25\ \mathrm{OD_{663.6}} - 2.55\ \mathrm{OD_{646.6}}$$

$$\mathrm{Chl.b\ (g/mL\ FW)} = 20.31\ \mathrm{OD_{646.6}} - 4.91\ \mathrm{OD_{663.6}}$$

$$\mathrm{Total\ chlorophyll\ content} = \mathrm{Chl.a\ (g/mL\ FW)} + \mathrm{Chl.b\ (g/mL\ FW)}$$

Plant tissue RNA extraction and reverse transcription

The expression of iron uptake-related genes was determined in the 1/2 MS, —Fe, –Fe + Fe_2O_3 + siderophore (100 ml of medium + 1 mL of crude extract, T2 treatment) treatment groups. Plants were harvested after they were transferred to different treatment media for 48 h. Plant RNA was extracted after quick freezing in liquid nitrogen and grinding according to the instructions of an RNA extraction kit (Accurate, Changsha, China). RNA was electrophoresed on a 1.5% (w/v) formaldehyde agarose gel. cDNA was synthesized from *Evo M-MLV* for qPCR.

Real-time quantitative PCR

For qRT–PCR analysis, SYBR qPCR Master Mix (Vazyme, Nanjing, China) was used. The expression levels of iron absorption-related genes and chlorophyll synthesis genes in the plants were analyzed with an ABI Prism 7900 instrument (Applied Biosystems, Foster City, America). Gene expression levels were determined according to the $2^{-\Delta\Delta Ct}$ method. The 1/2 MS treatment data were used to normalize the relative gene expression levels.

The primers for q-PCR were synthesized by Genscript Biotechnology Ltd. (Nanjing, China), and the sequences of the primers are shown in additional file 1.

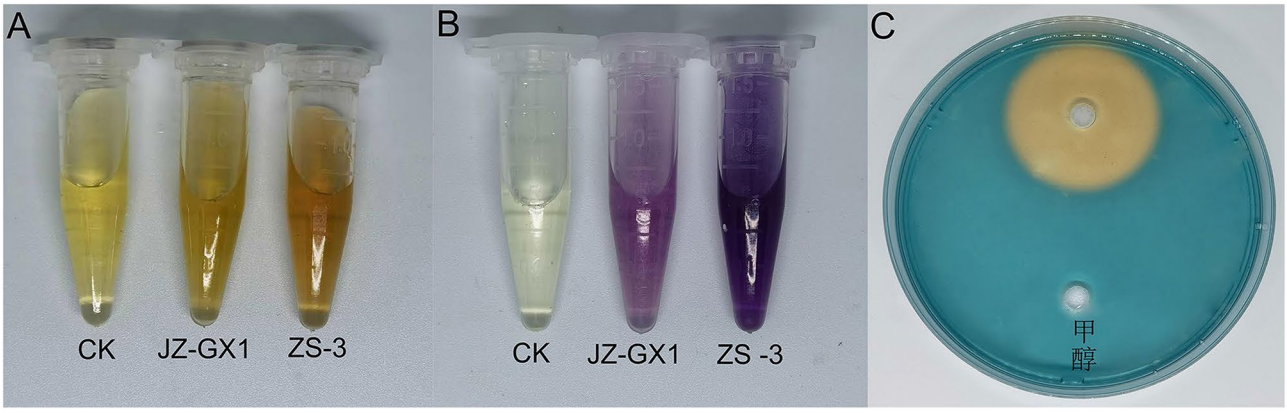

Fig. 1 Identification of siderophore types and crude extraction of siderophore from ZS-3 fermentation filtrate; (**A**) hydroxamic acid type was detected by $FeCl_3$ experiment; (**B**) Tetrazolium salt test to detect hydroxamic acid type; (**C**) Color reaction of 40 μL 100-fold *P. megaterium* ZS-3 siderophore crude extract cultured overnight in CAS plate under darkness

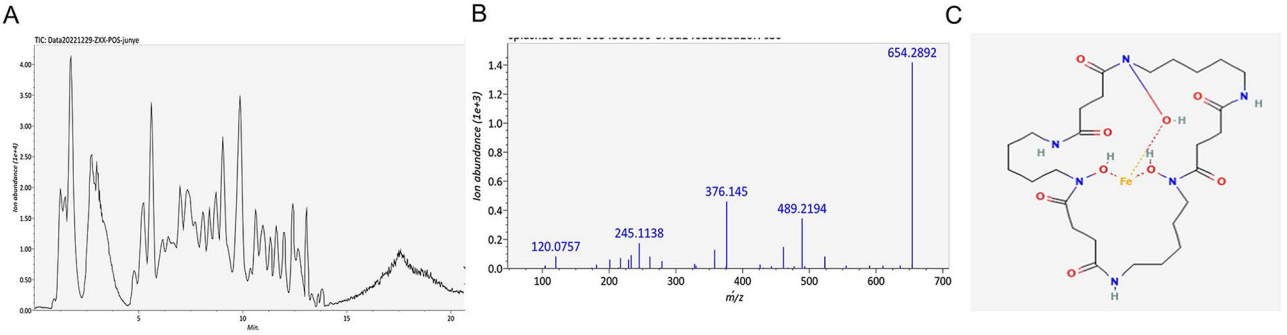

Fig. 2 Chromatogram and mass spectrum of crude extract of ZS-3 siderophore, and structure of ZS-3 siderophore. (**A**) Positive ion chromatogram of ZS-3 fermentation crude extract; (**B**) Positive ion mass spectrum of ZS-3 fermentation crude extract; (**C**) Structure of Ferrioxamine E [M + Fe-2 H] (structure provided by Pubchem (http://pubchem.ncbi.nlm.nih.gov) for Ferrioxamine E [M + Fe-2 H])

Data analyses

ANOVA and Duncan's multiple comparison tests were performed with IBM SPSS (version 22.0) (IBM Corporation, America), and the standard deviation of each mean was calculated ($p < 0.05$). All data in the graphs are presented as the mean ± standard deviation (SD) of at least three duplicate samples ($n = 3$). The charts were generated with GraphPad Prism 8.1 (GraphPad Software, China).

Results

Identification and crude extraction of siderophores from *P. megaterium*ZS-3

The type of siderophore in each medium filtrate was subjected to Arnow's test and $FeCl_3$, spectrophotometric and tetrazolium tests. The MTT and $FeCl_3$ tests revealed that ZS-3 produced hydroxamate-type siderophores; JZ-GX1 served as a positive control (Fig. 1(A) and (B)). Forty microliters of the fermentation filtrate of *P. megaterium* ZS-3, which was concentrated 100 times, was added to the CAS agar plate. After overnight culture in the dark, the crude extract of ZS-3 produced an obvious orange siderophore ring (Fig. 1(C)).

Characterization and quantification of siderophores from *P. megaterium*ZS-3

To explore the structure of the ZS-3 siderophore, the crude extract of *P. megaterium* ZS-3 was subjected to LC-MS/MS. A total of 377 chemicals were found in the crude fermentation liquid, and the chromatograms of all the substances are shown in Fig. 2(A). Positive ion chromatography–mass spectrometry was performed on the fermentation liquor, and there was a molecular ion peak at m/z 654.2892 ($[M + H]^+$) (Fig. 2(B)). The mass retention time of 8.95845 min was found to be that of Ferrioxamine E [M + Fe-2 H] after comparison with the secondary mass database.

Ferrioxamine E [M + Fe-2 H] is a kind of hydroxamic acid siderophore (Fig. 2(C)). Ferrioxamine E [M + Fe-2 H] contains three hydroxamic acid groups, in which the oxygen atom provides empty orbitals and the iron atom provides lone pairs, eventually forming a three-dimensional structure of a hexadentate octahedral complex. LC-MS/

MS was used to quantify the content of siderophores in the ZS-3 crude extract liquid, and the results showed that the content of Ferrioxamine E [M + Fe-2 H] was 137.98 μg/L at 36 h.

The *P. megaterium* ZS-3 siderophore promotes plant growth and alleviates iron deficiency-induced chlorosis

To evaluate the effect of the ZS-3 siderophore on the growth and iron deficiency tolerance of plants, in vitro iron deficiency stress experiments were carried out. Plants on 1/2 MS agar plates had a natural root distribution and green leaves (Fig. 3(A)). After treatment without iron for 6–7 days, the newly emerged leaves gradually turned yellow between the leaf veins. The taproots were slender and sensitive and detached easily when photos were taken (Fig. 3(B)). Compared with plants in the unstressed treatment, *A. thaliana* plants subjected to insoluble iron source stress caused by high contents of Fe_2O_3 had significantly thinner leaves and lower total fresh weights. Compared with the 1/2 MS treatment, the

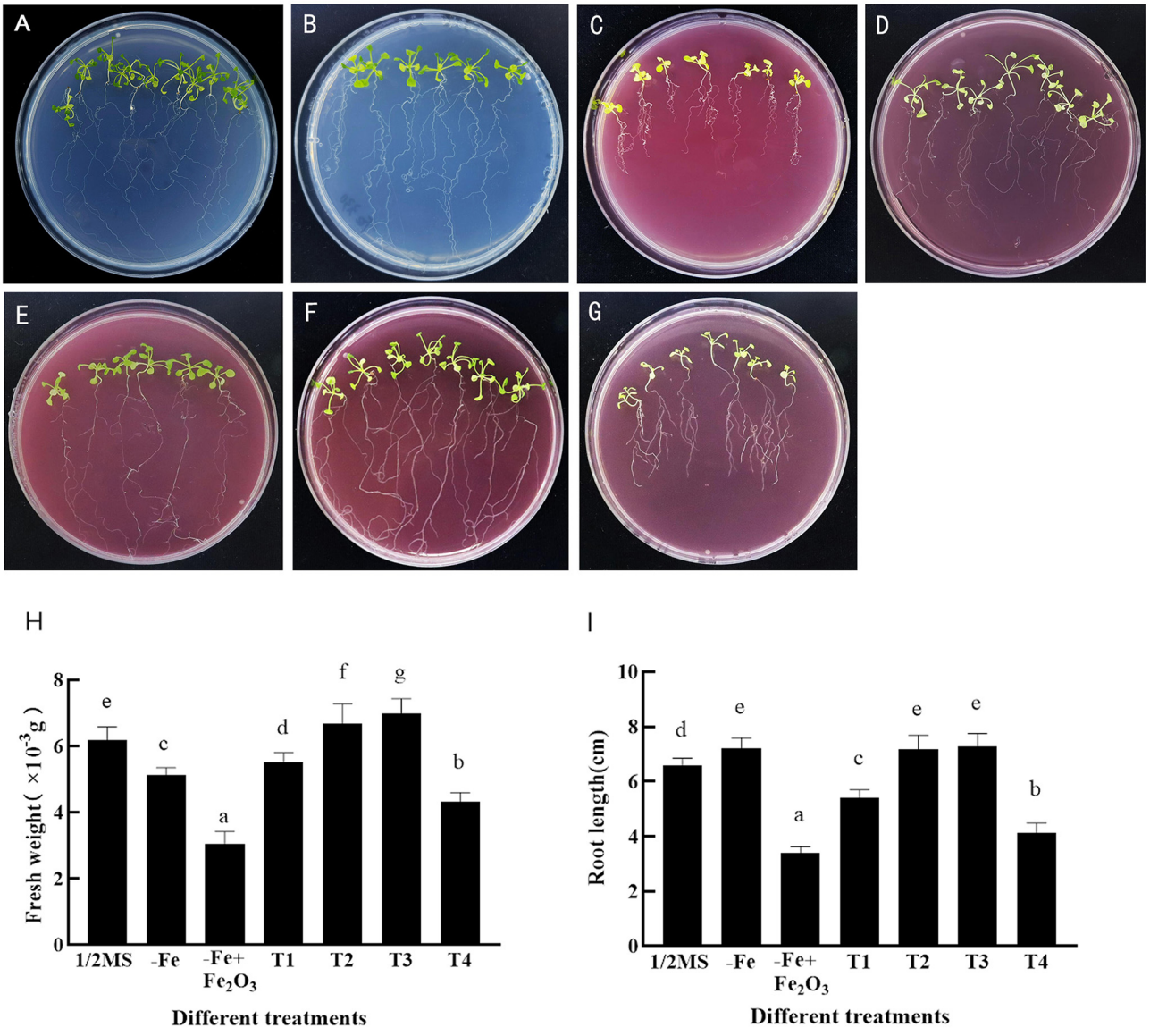

Fig. 3 (**A-G)** are plate diagram of *Arabidopsis thaliana* after 15 days of treatment with different concentrations of ZS-3 siderophore. (**A**) represents 1/2MS (Control); (**B**) Iron-deficient treatment (—Fe); (**C**) represents Fe_2O_3 added to iron-deficient medium (–Fe + Fe_2O_3, add 0.05 g Fe_2O_3 per 100mL medium); (**D**) represents T1 group treatment: T1 (500 μL ZS-3 siderophore added to 100 mL of –Fe + Fe_2O_3 medium; (**E**) represents the T2 group treatment T2 (1 mL of ZS-3 siderophore added to 100 mL of –Fe + Fe_2O_3 medium); (**F**) represents the T3 group treatment T3 (3 mL ZS-3 siderophore added to 100 mL of –Fe + Fe_2O_3 medium); (**G**) represents the T4 group treatment (5 mL ZS-3 siderophore added to 100 mL –Fe + Fe_2O_3 medium); (**H**) represents the effect of each different treatment on plant fresh weight; (**I**) represents the effect of each different treatment on plant root length, with different lowercase letters indicating significant differences between treatments ($P < 0.05$)

Fe_2O_3 treatment induced severe chlorosis of the leaves and dwarf plants (Fig. 3(C)). Compared with those in the control treatment, the total fresh weight (FW) and root length of the plants decreased by 136% and 133%, respectively, in the presence of Fe_2O_3. After inoculation with different contents of the ZS-3 siderophore, the plant roots lengthened, especially those in the T2 group, in which the leaf color was basically the same as that in the 1/2 MS group (Fig. 3(D-F)). However, inoculation with high contents of the ZS-3 siderophore in the insoluble iron treatment had a significant inhibitory effect on plant growth (Fig. 3(G)). In addition, the T2 treatment had good regreening effects, increasing the total fresh weight (FW) and root length of the plants by 132% and 118%, respectively, in the absence and presence of the ZS-3 siderophore. In the presence of Fe_2O_3, root growth was promoted in plants inoculated with the ZS-3 siderophore compared to that of uninoculated plants, but high amounts of the ZS-3 siderophore inhibited root length and fresh weight (Fig. 3(H-I)).

The *P. megaterium* ZS-3 siderophore promotes plant nutrient accumulation by enhancing plant photosynthesis

The expression levels of photosynthesis pigment-related genes, chlorophyll content and soluble protein content were quantified to investigate the potential role of the ZS-3 siderophore in the presence or absence of an insoluble iron source. The 1/2MS-Fe-treated plants had lower soluble protein and chlorophyll contents than the 1/2MS-treated plants, as the plants were under iron deficiency stress.

All the growth parameters of plants inoculated with Fe_2O_3were significantly lower than those of plants in the 1/2 MS treatment group, indicating that the plants could not directly absorb or utilize the insoluble iron source. Compared with those under the uninoculated ZS-3 siderophore treatment, the chlorophyll and soluble protein contents of the treated plants showed a continuous upward trend (Fig. 4(A) and (B)). Compared with those under Fe_2O_3 stress, the chlorophyll and soluble protein contents significantly increased in the ZS-3 siderophore-inoculated plants. Compared with those in the Fe_2O_3 treatment, the soluble protein and chlorophyll contents increased by 164% and 274%, respectively, in the T2 treatment group. The soluble protein content in the T2 treatment group increased by 88% compared to that in the 1/2 MS treatment group (Fig. 4(A) and (B)).

The expression of genes related to the chlorophyll synthesis pathways was examined in *A. thaliana* after ZS-3 siderophore inoculation, and the results showed that four key genes were activated to varying degrees by the ZS-3 siderophore. Compared to those in the 1/2MS treatment group, the *CHLD*, *CHLM* and *CHL* expression levels were suppressed in both the −Fe and Fe_2O_3 treatment groups, whereas there was no significant difference in *CHLG* expression. The Fe_2O_3 treatment had the lowest gene transcriptional activity among the four treatment groups, which is consistent with the plant phenotype and measured chlorophyll content (Fig. 4(C)). The chlorophyll synthesis genes were all upregulated in the Fe_2O_3 treatment group supplemented with the ZS-3 siderophore, suggesting that the ZS-3 siderophore enhances chlorophyll transcription and helps plants synthesize chlorophyll (Fig. 4(B) and (C)).

The *P. megaterium* ZS-3 siderophore is able to upregulate the expressions of iron uptake-related genes and increasing iron reductase activity

A. thaliana subjected to insoluble iron stress did not have a significantly lower active iron content than did plants in the T1 and T2 groups treated with the ZS-3 siderophore, but the T3 treatment significantly increased the active iron level (Fig. 5(A)). Ferric-chelate reductase activity was significantly inhibited in the −Fe and −Fe + Fe_2O_3 treatments but increased progressively with increasing siderophore content (Fig. 5(B)). FRO_2 encodes ferric reductase, which causes the reduction of Fe (III) to Fe (II) in high-valent iron chelates. *AHA2* encodes an H^+ ATPase that secretes H^+ to enhance Fe (III) solubility. The Fe (II) transporter protein encoded by *IRT1* transports reduced Fe (II) into the cell, and these three enzymes are essential for iron uptake in plants. In the −Fe and −Fe + Fe_2O_3 treatments, the iron transport-related genes FRO_2, *IRT1* and *AHA2* were suppressed compared to those in the plants in the 1/2 MS treatment group, but the expression levels of *FIT*, an iron transcriptional regulator, were not significantly downregulated (Fig. 5(C)). Compared to those in the 1/2MS treatment group, the FRO_2, *IRT1* and *AHA2* gene expression levels were upregulated by 489%, 383% and 29%, respectively, in the −Fe + Fe_2O_3 + ZS-3 siderophore treatment group, suggesting that the ZS-3 siderophore increases the abundance and activity of iron acquisition transcripts and contributes to iron uptake and utilization in plants.

The *P. megaterium* ZS-3 siderophore could increase the activity of protective enzymes and reducing the level of cellular reactive oxygen species

When subjected to adverse environmental stress, reactive oxygen species (ROS) levels increase dramatically, potentially causing severe damage to cell metabolism. The ROS level of plants in the 1/2 MS treatment group was significantly lower than that in the −Fe and −Fe + Fe_2O_3 treatment groups, suggesting that the plants were in a state of oxidative stress due to iron deficiency stress. Under conditions of insoluble iron source stress, plants inoculated with the ZS-3 siderophore exhibited greater peroxidase (POD) and superoxide dismutase (SOD) activity than

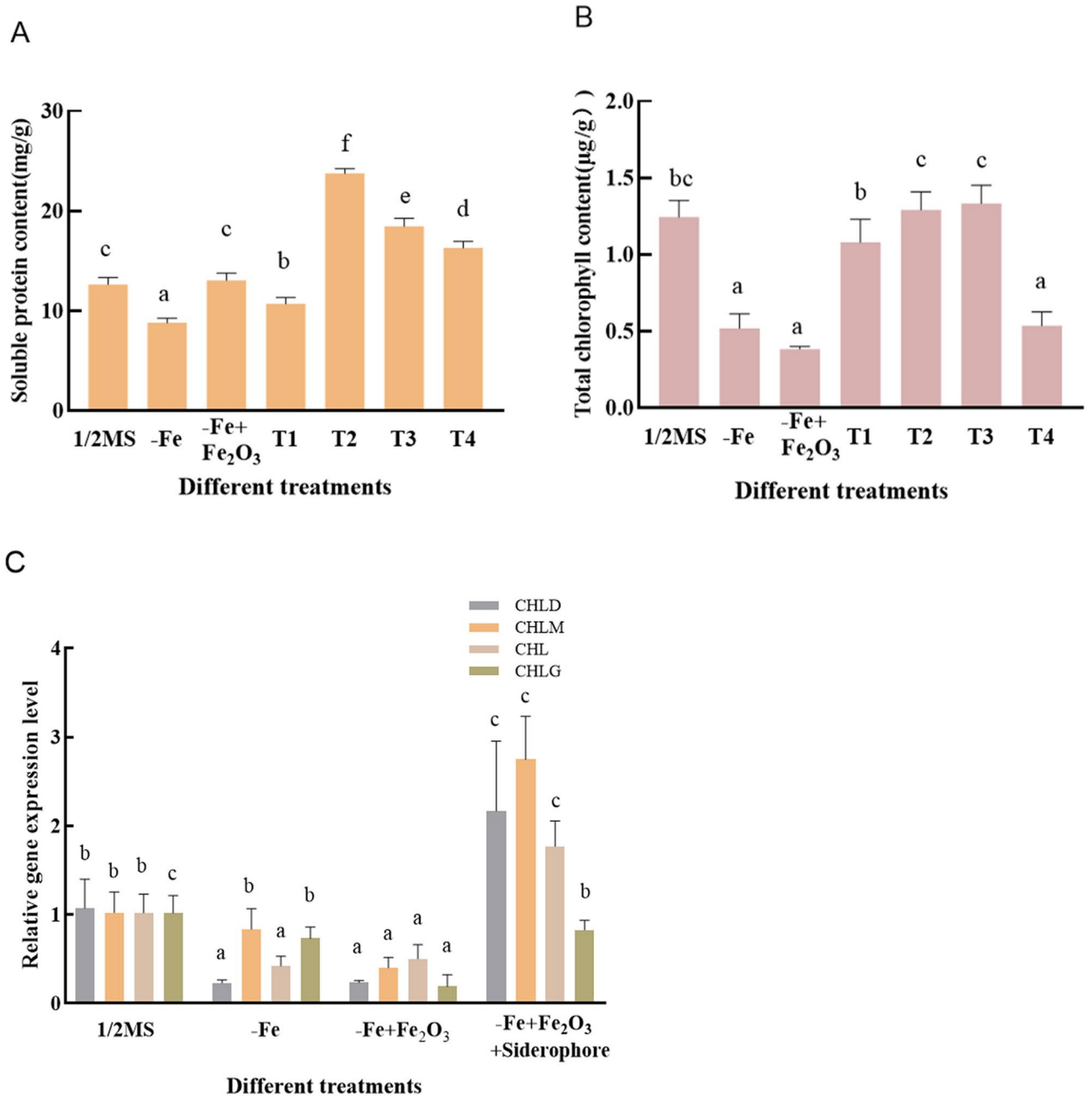

Fig. 4 (**A**) and (**B**) are the results of 1/2MS, −Fe, Fe_2O_3 (–Fe + Fe_2O_3), T1 (500 μL ZS-3 siderophore added to 100 mL of –Fe + Fe_2O_3 medium); T2 (1 mL ZS-3 siderophore added to 100 mL of –Fe + Fe_2O_3 medium); T3 (3 mL ZS-3 siderophore added to 100 mL of –Fe + Fe_2O_3 medium) and T4 (5 mL ZS-3 siderophore added to 100 mL of –Fe + Fe_2O_3 medium) treatments on plant soluble protein and chlorophyll content effects; (**C**) shows the expression of chlorophyll synthesis-related genes in samples treated with 1/2MS, –Fe, Fe_2O_3, and –Fe + Fe_2O_3 + Siderophore (T2 treatment). Different lowercase letters indicate significant differences between treatments ($P < 0.05$)

uninoculated plants, and inoculation with the ZS-3 siderophore significantly decreased the H_2O_2 and malondialdehyde (MDA) levels (Fig. 6(A) and (B)).

Compared to those in the uninoculated treatment, the POD and SOD activities of the plants in the siderophore-treated treatment group showed a continuous upward trend with increasing ZS-3 siderophore content, which significantly increased by 191% and 36.8%, respectively, in the T2 treatment group (Fig. 6(C) and (D)). This finding suggested that the ZS-3 siderophore increased plant antioxidant enzyme activities under insoluble iron stress, reduced the levels of ROS, and prevented the plants from being exposed to oxidative stress.

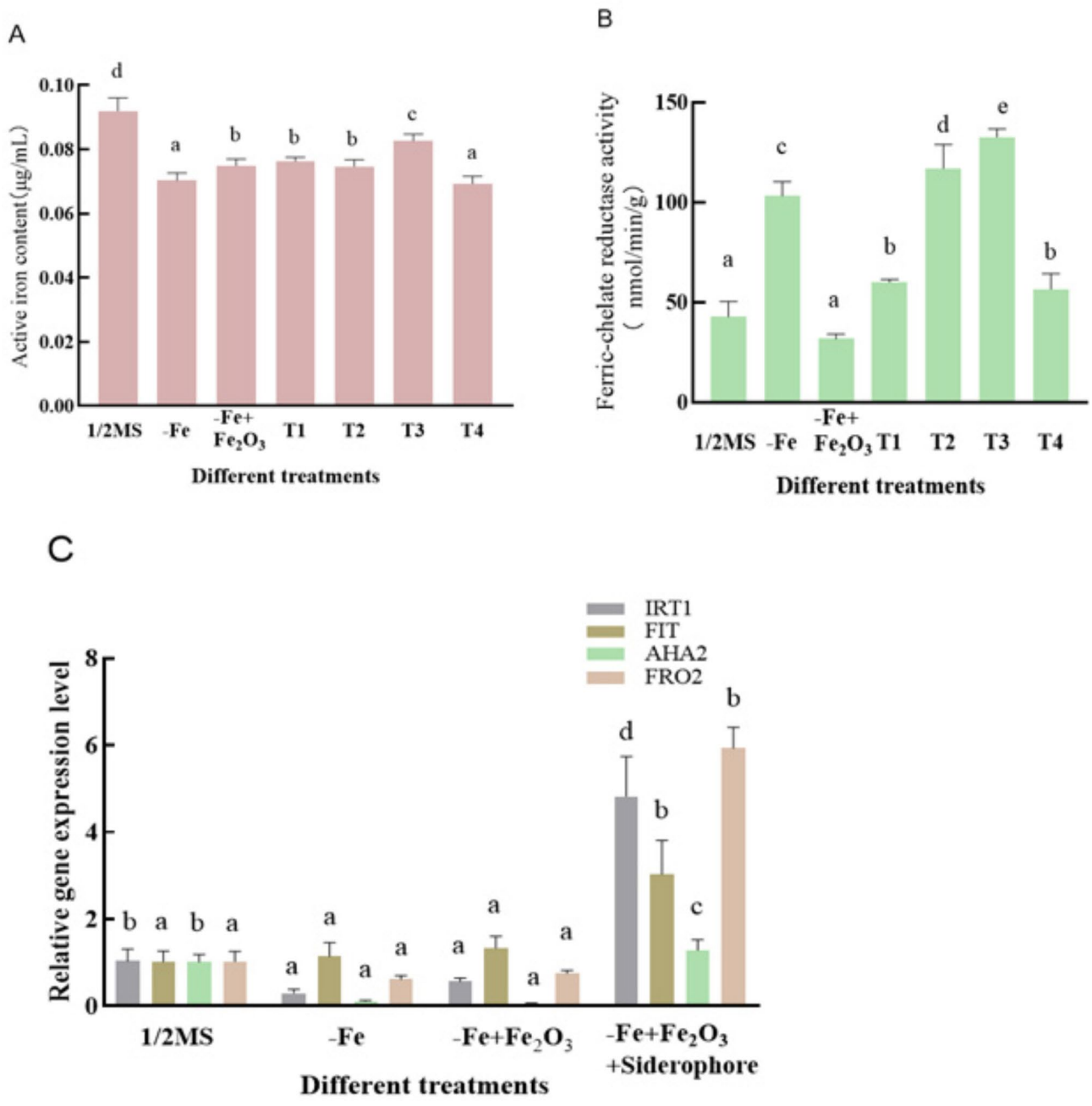

Fig. 5 (**A**) and (**B**) show the effect of 1/2MS, −Fe, Fe_2O_3 (–Fe + Fe_2O_3), T1 (500 µL ZS-3 siderophore added to 100 mL of –Fe + Fe_2O_3 medium), T2 (1 mL ZS-3 siderophore added to 100 mL of –Fe + Fe_2O_3 medium), T3 (3 mL ZS-3 siderophore added to 100 mL of –Fe + Fe_2O_3 medium) and T4 (5 mL ZS-3 siderophore added to 100 mL of –Fe + Fe_2O_3 medium) treatments on plant active iron content and ferric reductase activity. (**C**) shows the expression of iron uptake-related genes in samples treated with 1/2MS, –Fe, Fe_2O_3 and –Fe + Fe_2O_3 + Siderophore (T2 treatment). Different lowercase letters indicate significant differences between treatments ($P < 0.05$)

Discussion

In this study, *P. megaterium* ZS-3 Ferrioxamine E [M + Fe-2 H] was crudely proposed at 100 flod the concentration of the original fermentation broth following solid-phase extraction, and the structure of ZS-3 ferrioxamine was characterized for the first time. The results showed that the *P. megaterium* ZS-3 siderophore Ferrioxamine E [M + Fe-2 H] can increase the contact area between the root system and the environment to absorb more nutrients and enhance the iron uptake of the plant by increasing the expression of genes related to iron uptake. Taken together, these results suggest that the ZS-3 siderophore maintains normal plant growth by increasing the activities of antioxidant enzymes during

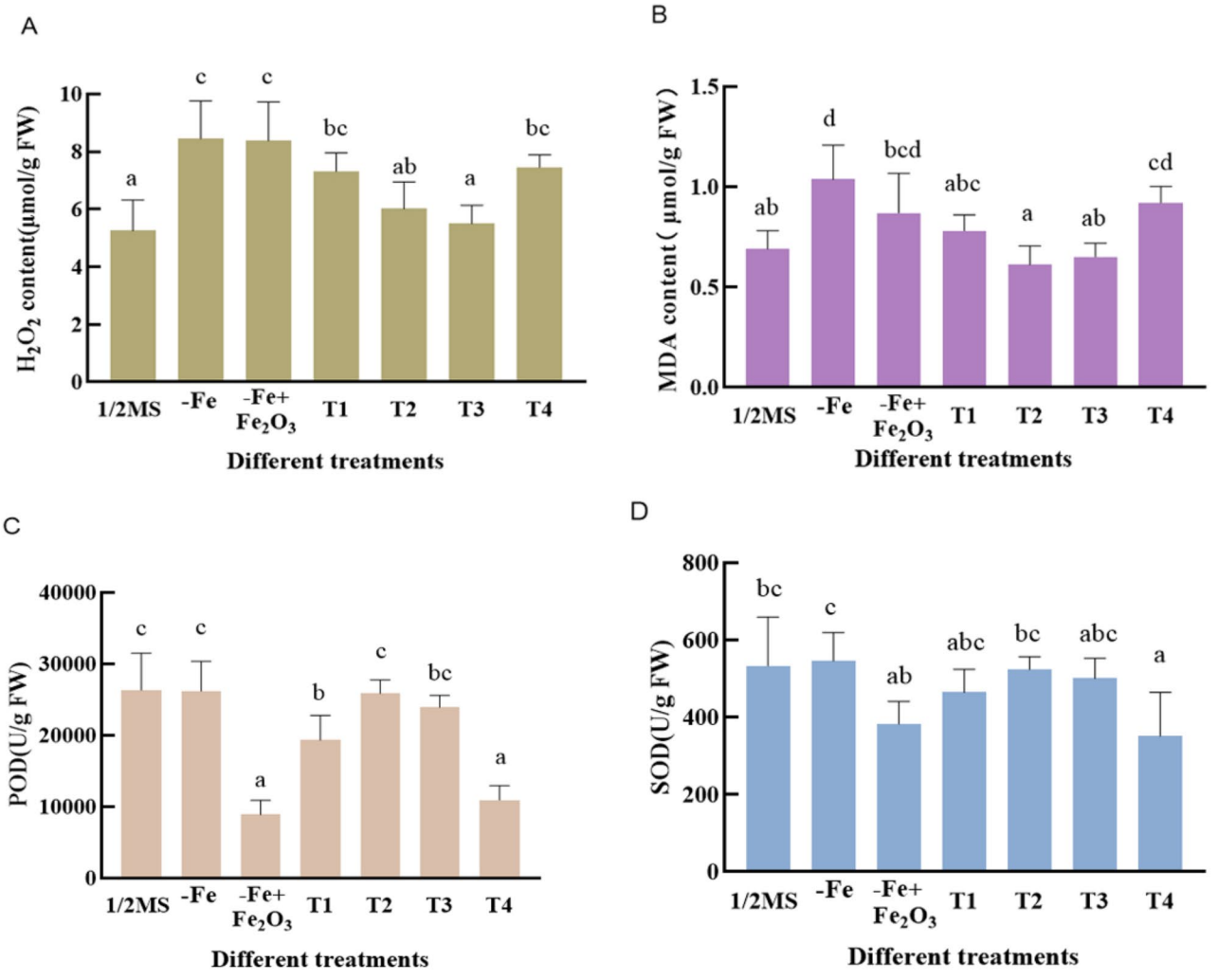

Fig. 6 Effects of different concentrations of ZS-3 siderophore on H_2O_2 (**A**), MDA (**B**) contents and Super Oxide Dismutase (SOD) (**C**), POD (**D**) activities in *Arabidopsis*. 1/2MS was used as the control, −Fe indicates iron-deficient treatment, and −Fe + Fe_2O_3 indicates addition of Fe_2O_3 to iron-deficient treatment. T1 (500 μL ZS-3 siderophore added to 100 mL of −Fe + Fe_2O_3 medium), T2 (1 mL ZS-3 siderophore added to 100 mL of −Fe + Fe_2O_3 medium), T3 (3 mL ZS-3 siderophore added to 100 mL of −Fe + Fe_2O_3 medium) and T4 (5 mL ZS-3 siderophore added to 100 mL of −Fe + Fe_2O_3 medium) with different lowercase letters indicate significant differences between treatments ($P < 0.05$)

Fe_2O_3 stress, promotes the acquisition of iron by increasing the activities of plant iron acquisition transcripts and iron chelating reductase, and enhances photosynthesis to increase the accumulation of nutrients through the upregulation of the expression of chlorophyll synthesis genes.

Growing evidence has shown that stress caused by insoluble iron sources seriously threatens plant growth, resulting in chlorosis and thinning of plant leaves [30]. Iron deficiency chlorosis can lead to tree weakness, increase the probability of plant pests and diseases, harm the growth of trees and even lead to tree death [31]. The foliar and root application of inorganic iron fertilizers is usually used to provide iron to plants. Hu Jing et al. proposed that the application of inorganic iron fertilizer had poor agronomic effectiveness [32], mainly because under aerobic conditions, iron ions are rapidly fixed in these two types of iron fertilizer, which rapidly blunts the iron deficiency stress response of plant roots, resulting in the downregulation of *FRO* and *IRT* genes and a decrease in ferric reductase activity [33]. This form of iron delivery prevents the plant from absorbing and utilizing iron and does not alleviate the plant's iron deficiency stress. Therefore, supplying plants with inorganic iron sources is equivalent to ineffective iron delivery.

Many studies have reported that PGPR have a progrowth effect under iron-deficient conditions [34, 35]. Siderophores are small molecule compounds secreted by organisms in response to iron-deficient environments for long-term iron acquisition, and most researchers have elucidated the mechanism of siderophore synthesis and secretion in these organisms and have demonstrated that

PGPR improve the uptake of iron in iron-deficient environments and aid in the acquisition of iron by plants. However, the important role of siderophores in plant iron acquisition, whether siderophores activate iron-regulated transcripts, whether they can improve root development, enhance photosynthesis, and enhance plant iron acquisition remain to be elucidated.

We used a normal treatment (1/2 MS), iron deficiency treatment (1/2 MS−Fe), and insoluble iron treatment (1/2 MS–Fe + Fe_2O_3) with the addition of four different concentrations of the ZS-3 siderophore of 1/2 MS–Fe + Fe_2O_3 to evaluate the effect of inoculation with the ZS-3 siderophore on the development and iron absorption of plants under Fe_2O_3 stress. Chlorophyll, the main photosynthetic pigment in plant leaves, is the fundamental substance for photosynthesis and is an important indicator of plant growth characteristics, physiological changes, and iron nutritional status. Compared with that of plants subjected to 1/2 MS, the chlorophyll content of plants in the 1/2 MS–Fe + Fe_2O_3 treatment decreased by 224.33%. However, in the group inoculated with siderophores (T3 group), compared with those in the Fe_2O_3 group, the chlorophyll and active iron contents increased by 71.2% and 9.27%, respectively. These results indicate that the ZS-3 siderophore promotes chlorophyll synthesis in plants. In angiosperms, represented by *A. thaliana*, 27 genes involved in 15 steps in the pathway from glutamyl-tRNA to chlorophylls a and b have been identified [36]. One subunit of magnesium chelatase is encoded by *CHLD*; the repression of *CHLM* expression reduces the accumulation of cystoid-associated proteins; the enzyme catalyzing the final step of chlorophyll a synthesis is encoded by *CHLG*; and chlorophyllate, an oxygenase, is encoded by *CHL*, which is responsible for the conversion of chlorophyll a to chlorophyll b [37]. These four genes are representative genes involved in chlorophyll biosynthesis in Arabidopsis [38]. The expressions of the four photosynthetic pigment genes were almost suppressed under Fe_2O_3 treatment, whereas compared with those under Fe_2O_3 treatment, the relative gene expressions of *CHLD*, *CHLM*, *CHL*, and *CHLG* increased by 0.892-, 0.854-, 0.715-, and 0.771-fold, respectively, after inoculation with Ferrioxamine E [M + Fe-2 H] (T2 treatment). This indicates that Ferrioxamine E [M + Fe-2 H] effectively enhanced the transcription level of photosynthetic pigments, improved plant photosynthesis and increased nutrient accumulation.

Reactive oxygen species (ROS) are natural byproducts of metabolism in living organisms and play an important role in cell signaling and metabolic homeostasis in vivo [39], and excessive ROS levels lead to the peroxidation of membrane lipids and damage to cell membranes [40]. SOD, POD, etc., are important reactive oxygen species-scavenging enzymes in living organisms that alleviate the damage to membrane lipids caused by oxidative stresses under adverse conditions. Iron is an important cofactor for the synthesis of many enzymes, the activities of POD and CAT are reduced under iron deficiency stress, and plant cells accumulate large amounts of superoxide radical (O^{2-}) and H_2O_2 [41]. This finding is consistent with that of Song [36], who reported that iron deficiency in peanuts caused severe accumulation of reactive oxygen species (ROS). In our study, inoculation with the ZS-3 siderophore Ferrioxamine E [M + Fe-2 H] effectively improved antioxidant enzyme activity, reduced the accumulation of reactive oxygen molecules, effectively alleviated the oxidative stress caused by iron deficiency, and enhanced the adaptability of plants to adverse conditions. Compared with inoculation with Fe_2O_3, inoculation with siderophores (T2 group) reduced the levels of H_2O_2 and MDA by 39.35% and 42.19%, respectively, while POD and SOD activities increased by 65.52% and 26.9%, respectively. Siderophores can enhance antioxidant enzyme activities, counteract adverse reactions caused by iron deficiency stress, and improve plant resistance to adverse conditions.

Shan [42] cultivated *Medicago sativa* in iron-deficient solution for 3 days, and the root length was significantly longer than that in the treatment group, with more fibrous roots and slight yellowing of the leaves. In the 1/2 MS–Fe treatment, the plant root length was also 8.3% longer than that in the 1/2 MS treatment, and the loss of green color between the veins of the new leaves may have been an adaptive response of the plants to the root-deficient environment to improve the efficiency of iron uptake by increasing the root length and uptake capacity to meet the demands of normal plant growth. In this study, compared with those in the 1/2 MS treatment, the length of the roots in the −Fe + Fe_2O_3 treatment decreased by 94.94%, the FCR activity decreased by 225.25%, and the activity of iron reductase (76.1%) increased in the ZS-3 siderophore treatment group inoculated under Fe_2O_3-insoluble iron stress (T3 treatment), resulting in better growth performance. In addition, the plant roots lengthened significantly with higher numbers of lateral roots, and the growth performance was even better than that of the 1/2 MS treatment. Furthermore, there was significantly higher iron reductase activity, which is consistent with the results of Aras S, Arikan S, and Youry Pii, who used bacterial inoculation to increase iron reductase activity [43–45]. We speculate that the elongation of plant roots and increased number of lateral roots increase the distribution of active sites of high iron reductase, thereby improving a plant's ability to absorb iron and improving the iron nutrition absorption status of the plant [46]. In addition, the –Fe + Fe_2O_3 treatment inhibited the expression of plant iron uptake-related genes, but after inoculation with the ZS-3 siderophore

Ferrioxamine E [M + Fe-2 H] (T2 treatment), the expression of related genes significantly increased. The relative gene expression levels of *IRT1*, *AHA2* and *FRO*$_2$ in the T2 treatment group were 8.45, 26.73 and 7.82 times greater, respectively, than those in the −Fe + Fe_2O_3 treatment group. These factors significantly enhanced the transcript abundance and activity of plant iron acquisition genes.

It was confirmed that the ZS-3 siderophore Ferrioxamine E [M + Fe-2 H] activated plant iron acquisition transcripts and increased the iron uptake-limiting enzyme activity, thus improving iron deficiency symptoms and enhancing photosynthesis. This treatment greatly improved the adaptive response of *A. thaliana* to mechanism I stress and significantly increased its resistance to iron deficiency and the total iron content of the plants. Therefore, Ferrioxamine E [M + Fe-2 H] can be used as a plant iron deficiency supplement in Fe_2O_3-rich soils and can effectively alleviate the symptoms of iron deficiency-induced chlorosis in plants.

Ferrioxamine is a member of the DFO family and is mainly secreted by Streptomyces. The DFO family is a typical class of hydroxamic acid-type siderophores. Eileen Schütze et al. [47] revealed that the extremely heavy metal-tolerant *Streptomyces mirabilis* P16B-1 secreted Ferrioxamine E, B, D and G from the DFO family at a uranium mine site heavily contaminated with heavy metals. In 1988, Ingrid Berner and others reported that ferrioxamine E is the main siderophore produced by *Herwinia herbicola* [48], and Zhang and others reported that ferrioxamine E is produced in seawater [49]. Between 1984 and 1995, several scientists discovered ferritins secreted by strains of *Priestia megaterium*, which belongs to the Schizokinen family [18, 25]. Ferrioxamine E [M + Fe-2 H] has not yet been reported in other bacterial species. The results of this experimental study indicate that Ferrioxamine E [M + Fe-2 H] was first discovered in *Priestia megaterium*.

In the DFO family, siderophores, such as deferrioxamine B, desferrioxamine G, and desferrioxamine mesylate, have mostly chain structures. Ferrioxamine E [M + Fe-2 H] is one of the few cyclic structures of siderophores in this family (other cyclic structures include desferrioxamine D2, desferrioxamine E, and ferrioxamine E) [49]. The binding constants of hydroxamate with iron range from 10^{22} to 10^{32}, and the chain structure has a weaker ability to bind Fe (III) than does the cyclic structure, resulting in a smaller stability constant. The stability constant of the combination of Ferrioxamine E and Fe (III) is 10^{32}, which is due to cyclization endowing the siderophore —Fe complex with greater stability and reducing its probability of enzymatic degradation [50–52].

In natural soil, Fe_2O_3 and plants are independent, Fe_2O_3 is a source of iron that cannot be directly absorbed and utilized by plants, and under Fe_2O_3 stress, plants are nutrient-deficient and grow slowly. After inoculation with Ferrioxamine E, the plant leaf color returns to green, and the root system expands, so siderophore acts as a "bridge" between Fe_2O_3 and the plant. In this study, we showed that Ferrioxamine E [M + Fe-2 H] activated the transcription of genes related to iron homeostasis in plants to promote iron acquisition, increase Fe (III) reductase activity and enhance iron utilization and that natural Fe (III) from insoluble iron sources formed a stable "ferrioxamine-Fe (III)" chelate. However, the mechanism by which plants utilize this chelate needs to be further investigated. One explanation is that plants can directly utilize this chelate through cytosolic complexes, while another explanation is that Fe (III) is reduced to Fe (II) by high-iron reducing enzymes in the roots, after which it dissociates from the complexes, and then the plants absorb and utilize Fe (II) [50, 53]. Currently, there is not enough information to support further discussion, so more detailed studies are needed to determine the mechanism of Fe transport.

In summary, the present study characterized the *P. megaterium* ZS-3 siderophore Ferrioxamine E [M + Fe-2 H] for the first time, laying the chemical foundation for the potential application of ferrioxamine E. The characterization, quantification and crude extraction of Ferrioxamine E [M + Fe-2 H] were also linked to the improvement of iron deficiency chlorosis in plants by Ferrioxamine E [M + Fe-2 H]. At the transcriptional level, it was revealed that Ferrioxamine E [M + Fe-2 H] activated the expressions of genes related to iron uptake and the key genes of photosynthetic pigments under iron deficiency conditions and that Ferrioxamine E [M + Fe-2 H] increased the activity of related enzymes to maintain normal life activities and mediate iron uptake. Ferrioxamine E [M + Fe-2 H] can be used as an iron deficiency inoculant in plants, and it was further demonstrated that Ferrioxamine E [M + Fe-2 H], a siderophore secreted by *P. megaterium* ZS-3, alleviated iron deficiency-induced chlorosis by enhancing the acquisition of iron via mechanism I, which lays a theoretical foundation for the siderophore-promoting mechanism under iron deficiency stress in plants.

Conclusion

The characterized Ferrioxamine E [M + Fe-2 H] in ZS-3 is first discovered in the *Priestia megaterium* and has played an essential role in alleviating chlorosis. Under the iron-deficiency status, Ferrioxamine E [M + Fe-2 H] is able to activate the expression of related genes at the transcriptional level to elevate chlorophyll and plant iron content, and depress ROS levels to maintain plant physiological metabolism. Overall, *Priestia megaterium* ZS-3 siderophore Ferrioxamine E [M + Fe-2 H] alleviated iron deficiency-induced chlorosis by enhancing the acquisition of iron via mechanism I.

Abbreviations

PGPR	Plant growth-promoting rhizobacteria
ZS-3	*Priestia megaterium* ZS-3
1/2 MS	One-half-strength Murashige and Skoog medium
POD	Peroxidase
FCR	Ferric-chelate reductase
SOD	Superoxide dismutase
H_2O_2	Hydrogen peroxide
MDA	Malondialdehyde
NBT	Nitrogen blue tetrazole
TCA	Trichloroacetic acid
Fe_2O_3	$-Fe+Fe_2O_3$
T1	500 μL ZS-3 siderophore added to 100 mL of $-Fe+Fe_2O_3$ medium
T2	1 mL ZS-3 siderophore added to 100 mL of $-Fe+Fe_2O_3$ medium
T3	3 mL ZS-3 siderophore added to 100 mL of $-Fe+Fe_2O_3$ medium
T4	5 mL ZS-3 siderophore added to 100 mL of $-Fe+Fe_2O_3$ medium
ROS	Reactive oxygen species
FW	Fresh weight

Supplementary Information

The online version contains supplementary material available at https://doi.org/10.1186/s12866-024-03669-8.

Additional file 1. Primer sequences related to iron uptake and photosynthetic pigment synthesis.

Acknowledgements
We thank the anonymous reviewers and editors for their helpful comments regarding the manuscript.

Author contributions
XXZ and JRY conceived and designed the research. LNS provided valuable advice on the data analysis and the experiments. HMS assisted with the statistical analysis. XXZ analyzed the data and drafted the manuscript. JRY revised the manuscript. All authors contributed to the article and approved the submitted version.

Funding
This work was financially supported by the State Forestry Administration Forestry Public Welfare Project of China (201304404).

Data availability
No datasets were generated or analysed during the current study.

Declarations

Ethics approval and consent to participate
Not applicable.

Consent for publication
Not applicable.

Competing interests
The authors declare no competing interests.

Received: 12 April 2024 / Accepted: 20 November 2024
Published online: 12 March 2025

References

1. Soares EV. Perspective on the biotechnological production of bacterial siderophores and their use. Appl Biochem Biotech. 2022;106(11):3985–4004.
2. Jeong J, Connolly EL. Iron uptake mechanisms in plants: functions of the *FRO* family of ferric reductases. Plant Sci. 2009;176(6):709–14.
3. Therby-Vale R, Lacombe B, Rhee SY, Nussaume L, Rouached H. Mineral nutrient signaling controls photosynthesis: focus on iron deficiency-induced chlorosis. Trends Plant Sci. 2022;27(5):502–9.
4. Terry N, Low G. Leaf chlorophyll content and its relation to the intracellular localization of iron. J Plant Nutr. 1982;5(4–7):301–10.
5. Yue Z, Chen Y, Hao Y, Wang C, Zhang Z, Chen C, et al. *Bacillus* sp. WR12 alleviates iron deficiency in wheat via enhancing siderophore and phenol-mediated iron acquisition in roots. Plant Soil. 2022;471(1):247–60.
6. Pei LP. Physiological role of iron in wheat and cloning study of *AVR9* gene. MS. Capital Normal University; 2002.
7. Santi S, Schmidt W. Dissecting iron deficiency-induced proton extrusion in *Arabidopsis* roots. New Phytol. 2009;183(4):1072–84.
8. Connolly EL, Campbell NH, Grotz N, Prichard CL, Guerinot ML. Overexpression of the FRO_2 ferric chelate reductase confers tolerance to growth on low iron and uncovers posttranscriptional control. Plant Physiol. 2003;133(3):1102–10.
9. Mukherjee I, Campbell NH, Ash JS, Connolly EL. Expression profiling of the Arabidopsis ferric chelate reductase (*FRO*) gene family reveals differential regulation by iron and copper. Planta. 2006;223(6):1178–90.
10. Robinson NJ, Procter CM, Connolly EL, Guerinot ML. A ferric-chelate reductase for iron uptake from soils. Nature. 1999;397(6721):694–7.
11. Ferreira Silva M, Silva H, Cunha A. Siderophore-producing rhizobacteria as a promising tool for empowering plants to cope with iron limitation in saline soils: a review. Pedosphere. 2019;29:409–20.
12. Santos S, Neto IFF, Machado MD, Soares HMVM, Soares EV. Siderophore production by *Bacillus megaterium*: Effect of growth phase and cultural conditions. Appl Biochem Biotech. 2014;172(1):549–60.
13. Hu X, Boyer GL. Isolation and characterization of the siderophore N-deoxyschizokinen from *Bacillus megaterium* ATCC 19213. Biometals. 1995;8(4):357–64.
14. Brozovic B. Iron transport and storage. Nature. 1976;260(5550):466–466.
15. Roskova Z, Skarohlid R, McGachy L. Siderophores: an alternative bioremediation strategy? Sci. Total Environ. 2022;819(3):153144.
16. Wilson MK, Abergel RJ, Arceneaux JEL, Raymond KN, Byers BR. Temporal production of the two *Bacillus anthracis* siderophores, petrobactin and bacillibactin. Biometals. 2010;23(1):129–34.
17. Wright W, Little J, Liu F, Chakraborty R. Isolation and structural identification of the trihydroxamate siderophore vicibactin and its degradative products from *Rhizobium leguminosarum* ATCC 14479 bv. Trifolii. Biometals. 2013;26(2):271–83.
18. Bhadrecha P, Singh S, Dwibedi V. A plant's major strength in rhizosphere: the plant growth promoting rhizobacteria. Arch Microbiol. 2023;205(5):165.
19. Aioub AAA, Elesawy AE, Ammar EE. Plant growth promoting rhizobacteria (PGPR) and their role in plant-parasitic nematodes control: a fresh look at an old issue. J Plant Dis Protect. 2022;129(6):1305–21.
20. Sreevidya M, Gopalakrishnan S. Direct and indirect plant growth-promoting abilities of *Bacillus* species on chickpea, isolated from compost and rhizosphere soils. Org Agr. 2017;7(1):31–40.
21. Sah S, Singh N, Singh R. Iron acquisition in maize (Zea mays L.) using Pseudomonas Siderophore. 3 Biotech. 2017;7(2):121.
22. Vary PS. Prime time for *Bacillus megaterium*. Microbiology. 1994;140(5):1001–13.
23. Shi L, Lu L, Ye J, Shi H. The endophytic strain ZS-3 enhances salt tolerance in *Arabidopsis thaliana* by regulating photosynthesis, osmotic stress, and ion homeostasis and inducing systemic tolerance. Front Plant Sci. 2022;13.
24. Gupta RS, Patel S, Saini N, Chen S. Robust demarcation of 17 distinct *Bacillus* species clades, proposed as novel *Bacillaceae genera*, by phylogenomics and comparative genomic analyses: description of *Robertmurraya kyonggiensis* sp. nov. and proposal for an emended genus *Bacillus* limiting it only to the members of the *subtilis* and *Cereus* clades of species. Int J Syst Evol Micr. 2020;70(11):5753–98.
25. Chuljerm H, Deeudom M, Fucharoen S, Mazzacuva F, Hider RC, Srichairatanakool S, et al. Characterization of two siderophores produced by *Bacillus megaterium*: a preliminary investigation into their potential as therapeutic agents. Bba-Gen Subj. 2020;1864(10):129670.
26. Shi HM, Lu LX, Wang Y, He LN, Wang XY, Ye JR. Effects of five growth-promoting microbial fertilisers on the growth and the fruit quality of Vitis vinifera, Molecular Plant Breeding. 2022;1–9.
27. Baakza A, Vala AK, Dave BP, Dube HC. A comparative study of siderophore production by fungi from marine and terrestrial habitats. J Exp Mar Biol Ecol. 2004;311(1):1–9.
28. Kumar D, Yusuf MA, Singh P, Sardar M, Sarin NB. Modulation of antioxidant machinery in α-tocopherol-enriched transgenic *Brassica juncea* plants tolerant to abiotic stress conditions. Protoplasma. 2013;250(5):1079–89.
29. Azarmi F, Mozafari V, Abbaszadeh Dahaji P, Hamidpour M. Biochemical, physiological and antioxidant enzymatic activity responses of pistachio seedlings

treated with plant growth promoting rhizobacteria and zn to salinity stress. Acta Physiol Plant. 2015;38(1):21.
30. Sultana S, Alam S, Karim MM. Screening of siderophore-producing salt-tolerant rhizobacteria suitable for supporting plant growth in saline soils with iron limitation. J Agr Food Res. 2021;4(29):100150.
31. Hua F. Effects of phosphate and bicarbonate concentrations on iron uptake in *Cinnamomum camphora* seedlings. M.S. Zhejiang University; 2009.
32. Hu J. Corrective effect and evaluation of iron oxide nanoparticles (γ-Fe_2O_3 NPs) on *Citrus reticulata Blanco* iron-deficiency chlorosis disease. M.S. Wuhan University of Technology; 2017.
33. Lopez-Millan AF, Morales F, Gogorcena Y, Abadía A. Iron resupply-mediated deactivation of Fe-deficiency stress responses in roots of sugar beet. Aust J Plant Physiol. 2001;28(3):171–80.
34. Delaporte-Quintana P, Lovaisa NC, Rapisarda VA, Pedraza RO. The plant growth promoting bacteria *gluconacetobacter diazotrophicus* and *Azospirillum brasilense* contribute to the iron nutrition of strawberry plants through siderophores production. Plant Growth Regul. 2020;91(2):185–99.
35. Sun Y, Wu J, Shang X, Xue L, Ji G, Chang S, et al. Screening of siderophore-producing bacteria and their effects on promoting the growth of plants. Curr Microbiol. 2022;79(5):150.
36. Song Y, Dong Y, Tian X, Wang W, He Z. Mechanisms of exogenous nitric oxide and 24-Epibrassinolide alleviating chlorosis of peanut plants under iron deficiency. Pedosphere. 2018;28(6):926–42.
37. Beale Sl. Green genes gleaned. Trends Plant Sci. 2005;10(7):309–12.
38. Lu X, Sun D, Zhang X, Hu H, Kong L, Rookes JE, et al. Stimulation of photosynthesis and enhancement of growth and yield in *Arabidopsis thaliana* treated with amine-functionalized mesoporous silica nanoparticles. Plant Physiol Bioch. 2020;156:566–77.
39. Ma D. Screening of sweet sorghum germplasm resistant to petroleum hydrocarbon pollution and its responses to phenanthrene stress. M.S. Shandong Agricultural University. 2023.
40. Guo Y, Jiang J, Pan Y, Yang X, Li H, Li H, et al. Effect of high O_2 treatments on physiochemical, lycopene and microstructural characteristics of cherry tomatoes during storage. J Food Process Pres. 2019;43(11):e14216.
41. Hassan N, Ebeed H, Aljaarany A. Exogenous application of spermine and putrescine mitigate adversities of drought stress in wheat by protecting membranes and chloroplast ultra-structure. Physiol Mol Biol Pla. 2020;26(2):233–45.
42. Shan HY. The effects of salt alkali and iron stress on the physiology and related gene expression of Medicago sativa. 2017; M.S. Harbin Normal University.
43. Aras S, Arikan Ş, Ipek M, Esitken A, Pirlak L, Dönmez M, et al. Plant growth promoting rhizobacteria enhanced leaf organic acids, FC-R activity and Fe nutrition of apple under lime soil conditions. Acta Physiol Plant. 2018;40(6):120.
44. Arikan Ş, Esitken A, Ipek M, Aras S, şahin M, Pirlak L, et al. Effect of plant growth promoting rhizobacteria on Fe acquisition in peach (*Prunus Persica* L) under calcareous soil conditions. J Plant Nutr. 2018;41(17):2141–50.
45. Pii Y, Marastoni L, Springeth C, Fontanella MC, Beone GM, Cesco S, et al. Modulation of Fe acquisition process by *Azospirillum brasilense* in cucumber plants. Environ Exp Bot. 2016;130(10):216–25.
46. Kong WL. The effect and mechanism of *Rahnella aquatilis* JZ-GX1 alleviating iron deficiency chlorosis in *Cinnamomum camphora*. PhD. Nanjing Forestry University. 2022.
47. Schütze E, Ahmed E, Voit A, Klose M, Greyer M, Svatoš A, et al. Siderophore production by streptomycetes-stability and alteration of ferrihydroxamates in heavy metal-contaminated soil. Environ Sci Pollut Res Int. 2015;22(24):19376–83.
48. Berner I, Konetschny-Rapp S, Jung G, Winkelmann G. Characterization of ferrioxamine E as the principal siderophore of *Erwinia herbicola* (Enterobacter agglomerans). Biol Met. 1988;1(1):51–6.
49. Zhang L, Yuan D-X, Fang K, Liu B-M. Determination of siderophores in seawater by high performance liquid chromatography-tandem mass spectrometry coupled with solid phase extraction. Chin J Anal Chem. 2015;43(9):1285–90.
50. Hördt W, Römheld V, Winkelmann G. Fusarinines and dimerum acid, mono- and dihydroxamate siderophores from *Penicillium Chrysogenum*, improve iron utilization by strategy I and strategy II plants. Biometals. 2000;13(1):37–46.
51. Robin A, Vansuyt G, Hinsinger P, Meyer J, Briat J-F, Lemanceau P. Chapter 4 iron dynamics in the rhizosphere. Adv Agron. 2008;99:183–225.
52. Winkelmann G. Microbial siderophore-mediated transport. Biochem Soc T. 2002;30(4):691–6.
53. Wu JL. Screening and identification of siderophore-producing bacteria and their growth-promoting effects on test plants. 2020.M.S. Lanzhou Jiaotong University.

Publisher's note